Linearized Modulator for Suboctave-Bandpass Optical Analog Links

Gary E. Betts

Abstract— **The spurious-free dynamic range of a suboctave externally modulated optical analog link can be improved (to >140 dB Hz$^{4/5}$) with modest received optical power and little noise figure penalty by using a simple linearized modulator. Its design consists of two standard Mach–Zehnder interferometric modulators in series, and so can operate at microwave frequencies. This paper develops standardized measures of linearized modulator performance, and uses them to evaluate the modulator; link examples are also given. A simple experiment verifies the basic theoretical predictions.**

I. Introduction

OPTICAL analog links are useful for a variety of applications, including antenna remoting, phased-array antenna control, and cable TV. Many of these applications (the notable exception being cable TV) involve bandwidths of less than one octave, so second-order distortion is not a consideration. Most previous work on techniques for enhancing the dynamic range of analog links, beyond that obtainable with a single Mach–Zehnder (MZ) interferometric modulator, has focused on the cable TV application where link noise figure is not important and both second- and third-order distortion must be controlled. For suboctave-bandpass links, second-order distortion is not a problem. For many applications, noise figure *is* a prime consideration. At microwave frequencies, detectors cannot handle more than a few milliamperes of dc current because of their small size. Thus, the criteria for a good modulator for microwave bandpass links are significantly different than for a good cable TV modulator. We have optimized modulator design to minimize third-order distortion and average optical power while maximizing output signal-to-noise ratio at a fixed electrical power input. The result is a simple modulator that gives better link noise figure and lower average optical power output than a single MZ biased at quadrature, while also giving a third-order dynamic range as large as any linearized modulator design.

Most externally modulated optical analog links use a single MZ modulator, as shown in Fig. 1. The modulator is biased at quadrature, $\phi_1 = 90°$ (the bias point ϕ_1 is the quiescent optical phase difference between arms) to give zero second-order distortion and maximum link electrical gain. The modulator's average (dc) optical transmission is 0.5 at this bias point. This gives a link with high enough performance for many applications [1]. We will use this type of link as a standard of comparison. Its main performance problems are that the third-order distortion is too large for some applications, the noise figure is high at microwave frequencies, and high performance requires high detector current.

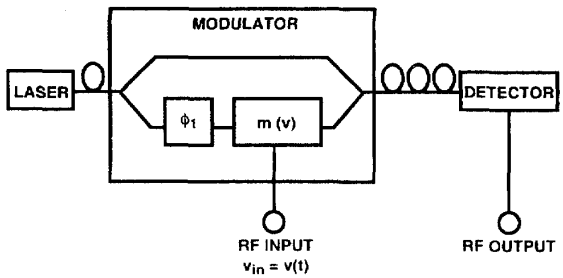

Fig. 1. Diagram of optical analog link using interferometric modulator.

The modulator described in this paper brings together two separate lines of development: operation of the single MZ modulator at a bias point close to its transmission minimum, and linearization of the electrooptic modulator. By using a bias point in the range $90° < \phi_1 < 180°$ [2]–[4], the link noise figure and the average detector current can be reduced, with the cost of high second-order distortion. These advantages come about because the primary link noise sources fall faster than the link gain as the bias point is increased from 90° [4]. (It may appear that optical power is somehow wasted by picking a modulator configuration or bias point that results in only a small fraction of the input power appearing as average output power. This is not the case. The key measures of link performance, the noise figure and dynamic range, depend on the signal-to-noise *ratio*, so reduction of signal power (i.e., modulated optical power) does not matter as long as the noise is reduced by a larger factor.)

There are many modulator designs that produce less third-order distortion than the single MZ [5]–[12]. These generally are complex, difficult to control, and/or cause significant noise figure penalties. Series connection of an MZ with a second MZ of reduced extinction (i.e., an optical power imbalance between arms so that the transmission is never zero) [10]–[12] produces a linearized modulator that retains the design advantages of the MZ modulator and avoids the optical power splitting/combining difficulties of the parallel MZ [7]. These reduced-extinction series MZ designs require two critical control adjustments and incur a noise figure penalty of approximately 6 dB compared to a single MZ,

Manuscript received April 1, 1994; revised June 20, 1994. This work was supported by the Department of the Air Force.

The author is with Lincoln Laboratory, Massachusetts Institute of Technology, Lexington, MA 02173-9108 USA.

IEEE Log Number 9405425.

mainly due to the constraint of simultaneously minimizing both second- and third-order distortion.

We have found that when there is no requirement for minimization of second-order distortion, the series connection of two Mach–Zehnder interferometers (series MZ) can be simplified and its performance improved substantially over the designs summarized above. First, there is no requirement for reduced extinction on one of the modulators, so two standard (equal power in arms) MZ's can be used. Second, there is only one critical adjustment, which is the bias point on one of the modulators. Third, the noise figure of a link using this type of modulator can actually be lower than the noise figure of a link using a single MZ biased at quadrature. Finally, the bias points of the modulators can be set so that the average detector current is substantially reduced while preserving link performance, in a manner similar to the use of a bias point $90° < \phi_1 < 180°$ on a single MZ.

Evaluation of the performance of a new modulator design is difficult because of the many different systems in which it could be used, and therefore the many different performance measures that may be important. We will give normalized modulator performance measures that should answer most performance questions, and then use these measures to compare the series MZ to the single MZ and to the dual parallel MZ [7], which is perhaps the best-understood linearized modulator. We will also give results for the performance advantage this modulator provides in a simple high-performance analog link (Bridges and Schaffner [6] give results for some other modulator types using an analog link for comparison). We will not consider the use of a preamplifier in this paper; however, this is a nontrivial issue and an analysis of it can be found in [13].

II. Theory

A. Modulator Performance Characterization

An electrooptic modulator has an electrical-to-optical transfer function given by

$$\frac{P_{out}}{P_{in}} = f[m(v)] \tag{1}$$

where P_{in} and P_{out} are the input and output optical power, an m is a dimensionless, linear function of the applied voltage v. The output current from the link detector is $i_0 f[m(v)]$, where i_0 is the current when the modulator is set to maximum transmission ($f = 1$); i_0 includes the laser power, optical losses, and detector responsivity. For small signals ($m \ll 1$), the transfer function (1) can be expanded in terms of m as [14]

$$f(m) = \sum_n c_n m^n. \tag{2}$$

For an input signal

$$m = \sum_p m_p \sin \omega_p t \tag{3}$$

the link output current is

$$i = i_{avg}\left(1 + \sum_p M_p \sin \omega_p t + \sum_j M_j \sin \omega_j t\right) \tag{4}$$

where M represents the optical modulation depth and the ω_j are spurious frequencies, present in the output but not in the input. The average detector current is $i_{avg} = i_0 c_0$. The optical modulation depths of the fundamental signals are $M_p = m_p|c_1|/c_0$. Spurious frequencies are generated whenever $c_n \neq 0$ for any $n \geq 2$. The $c_2 m^2$ term produces second-order distortion, the $c_3 m^3$ term produces third-order distortion, the $c_5 m^5$ term produces fifth- and third-order distortion, and so on. The third-*order* distortion produced by the $c_5 m^5$ term is fifth *degree* in m, however, and as such is much smaller than the third-order distortion from the $c_3 m^3$ term for small m.

We are interested in minimizing third-order distortion in this paper. To quantify this, we will assume the input signal (3) consists of two frequencies of equal amplitude and look at the third-order intermodulation output signal. The figure of merit for the modulator in this case is the third-order-intercept optical modulation depth M_{IP3}, which is the optical modulation depth at which the fundamental and third-order-intermodulation signals have the same modulation depth (when extrapolated from small signals). M_{IP3} and n, the degree of the lowest term that has $c_n \neq 0$ for n odd, are sufficient to characterize the third-order distortion of the modulator. M_{IP3} can be expressed in terms of the coefficients c_n (this is done by Halemane and Korotky [14] using c_n up to $n = 3$), or M_{IP3} and n can be obtained directly from the modulator transfer function by use of a Fourier transform (as will be done in this paper).

The rms electrical power output from the link for any one of the frequency components in (4) is

$$p = \frac{1}{2} i_{avg}^2 M^2 R_d \tag{5}$$

where R_d is the detector load resistance; the link's output third-order-intercept point is

$$p_{IP3} = \frac{1}{2} i_{avg}^2 M_{IP3}^2 R_d. \tag{6}$$

The output noise (in a 1 Hz bandwidth) from the link is

$$N_o = F_R kT + 2e i_{avg} R_d + \mathcal{R} i_{avg}^2 R_d \tag{7}$$

where F_R is the receiver noise figure, k is Boltzmann's constant, T =290 K is the standard noise temperature, e is the electronic charge, and $\mathcal{R}$ is the optical relative intensity noise (RIN) at the detector. The first term is the receiver noise, the second is the shot noise, and the third is the noise due to optical intensity noise. The third-order-intermodulation-free dynamic range is

$$DR = \left(\frac{p_{IP3}}{N_o B}\right)^{(n-1)/n} = \left(\frac{2F_R kT}{i_0^2 R_d}\frac{1}{c_0^2 M_{IP3}^2} + \frac{4e}{i_0}\frac{1}{c_0 M_{IP3}^2} + 2\mathcal{R}\frac{1}{M_{IP3}^2}\right)^{-(n-1)/n} B^{-(n-1)/n} \tag{8}$$

where B is the noise bandwidth and n is the degree of the dependence of the third-order-intermodulation signal power on the input signal power. To calculate the link gain and noise figure, we need to define a relation between m_p and the

TABLE I
COMPARISON OF MODULATOR PERFORMANCE FOR VARIOUS NOISE SOURCES (USING DIMENSIONLESS MODULATOR FIGURES OF MERIT)

NOISE SOURCE			RECEIVER		SHOT		RIN	
PERFORMANCE MEASURE	2ND-ORDER DISTORTION	3RD-ORDER SLOPE	DR(1)	F	DR	F	DR	F
FIGURE OF MERIT		n	$c_0^2 M_{IP3}^2$	$\frac{1+r^2}{c_1^2}$	$c_0 M_{IP3}^2$	$c_0 \frac{1+r^2}{c_1^2}$	M_{IP3}^2	$c_0^2 \frac{1+r^2}{c_1^2}$
SINGLE MZ, ϕ_1=90°	NO	3	2	4	4	2	8	1
SINGLE MZ, 90°≤ϕ_1<180° (2)	YES	3	2	4	8	1	∞	0
DUAL PARALLEL MZ	NO	5	0.34	45	0.67	22.6	1.35	11.2
SERIES MZ(2)	YES	5	0.39	16	8	1	∞	0

(1) DR refers to third-order-intermodulation-free dynamic range.
(2) Single MZ, $90° \leq \phi_1 < 180°$ and Series MZ are optimized differently for receiver noise than for shot noise and RIN.

electrical input power. We will define the modulator response K as

$$K = \frac{m_p^2}{p_{in}} \tag{9}$$

where p_{in} is the rms electrical input power at the frequency ω_p. The noise figure is then

$$F = \frac{N_0}{GkT} = \frac{2F_R}{i_0^2 R_d}\frac{1}{Kc_1^2} + \frac{4e}{i_0 kT}\frac{c_0}{Kc_1^2} + \frac{2\mathcal{R}}{kT}\frac{c_0^2}{Kc_1^2} \tag{10}$$

where G is the link electrical gain.

Equations (8) and (10) relate the key link performance measures to the modulator parameters c_0, c_1, K, n, and M_{IP3}. The parameters to optimize depend upon which noise source is the limiting factor in a given application. We will use these performance measures to evaluate the series MZ modulator below. The above treatment applies to any type of modulator. The parameters c_0, n, and M_{IP3} are independent of the choice of $m(v)$; however, c_1 and K do depend on how $m(v)$ is chosen. When comparing the noise figure of different modulator types, $m(v)$ must be chosen in a consistent way for all if c_1 and K are to be directly comparable. In the remainder of this paper, we will consider only modulators built up out of MZ modulators, so we will be able to reduce Kc_1^2 to a single factor.

In a single MZ modulator (as shown in Fig. 1), an applied voltage produces an optical phase difference between its arms, which in turn produces intensity modulation when the light from the two arms is combined. A signal $v = v_p \cdot \sin(\omega t)$ produces a modulation of the phase difference of $m_p \cdot \sin(\omega t)$, where we are now defining $m_p = \pi v_p / v_\pi$ as the phase modulation depth (PMD); v_π is the voltage required to change the phase difference between arms by π. With this definition, for small signals, a single MZ produces an optical modulation depth $M_p = m_p$. We define the response of a single MZ as $K_s = m_p^2/p_{ins}$, where p_{ins} is the RF power input to the single modulator. For a dual MZ (either series or parallel), we assume the second MZ has the same K_s, but is driven with r^2 as much electrical power, so it has a PMD of $r \cdot m_p$ (this is diagrammed for the series MZ in Fig. 2). With these definitions, the

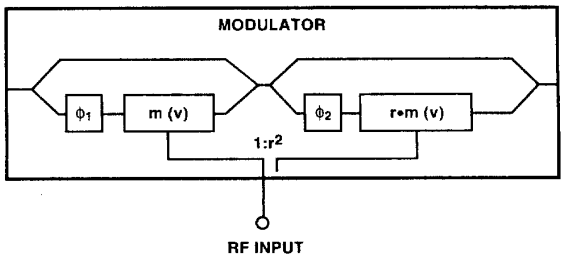

Fig. 2. Series Mach–Zehnder interferometer. Optical power is equally split at each Y-branch. Electrical power is split in ratio $1: r^2$ between interferometers.

response of a modulator consisting of a combination of one or two MZs is

$$K = K_s \frac{1}{1+r^2}. \tag{11}$$

This can be substituted into (10) to get the modulator figures of merit shown in Table I. Table I shows the effects of how the MZ's are arranged and biased; the link parameters and K_s are not shown because improvements in them would improve all designs equally.

B. Simplified Series Mach–Zehnder Modulator

The reduced third-order distortion of the series MZ can be intuitively understood by considering the contributions to the cubic term of the transfer function. There is a contribution from the cubic term of each MZ individually, and there is also a contribution from the product of the linear term of one modulator with the quadratic term of the other. The modulator parameters can be chosen so that the cubic product terms cancel the cubic terms from the individual modulators, while the linear terms from the individual modulators add to maximize the fundamental.

The detector output current from a link using the dual series MZ is

$$i = \frac{1}{4} i_0 \{1 + \cos[\phi_1 + m(v)]\}\{1 + \cos[\phi_2 + r \cdot m(v)]\} \tag{12}$$

where ϕ_1 and ϕ_2 are the bias points, and other quantities have been defined above. This can be expanded in powers of m as described by (2). The third-order distortion can be reduced by requiring $c_3 = 0$ (this solution method has been used on other linearized modulators [7], [8]). There are three free variables, r, ϕ_1, and ϕ_2, so two can be chosen to optimize other aspects of modulator performance, and the third can be determined from the $c_3 = 0$ condition. (It is not possible, however, to use the extra degrees of freedom to simultaneously satisfy $c_2 = 0$ with this simplified version of the dual series MZ.) The relative phase of the RF signal applied to the two modulators must be the same (at high frequencies, the optical propagation time between the modulators must be considered), i.e., r must be a real number.

Fig. 3 shows how a particular series MZ design compares to a single MZ biased at quadrature. When the series MZ is designed so $c_3 = 0$, the third-order-intermodulation signals fall as the fifth power of the input power, which gives the series MZ a larger dynamic range. Because of this property, the amount of dynamic range improvement depends upon the dynamic range of the single MZ link: links that have a large dynamic range with a single MZ will show greater improvement in dynamic range when a series MZ is used than will links with a small dynamic range. This is easiest to see in Fig. 3 by considering a larger noise bandwidth, which would move the noise floor upward; it is also true when the dynamic range is changed by changing the nonmodulator-related link design parameters evident in (8), e.g., i_0. (Links with higher dynamic range have the noise floor at smaller PMD, where the difference between third- and fifth-degree dependence is greater. To calibrate Fig. 3, $m_p = 1$ at +10 dBm input for the single MZ, and $r \cdot m_p = 1$ at +10.4 dBm for the series MZ.) Thus, the amount of dynamic range improvement available from this modulator (or any designed using the $c_3 = 0$ scheme) depends critically on the parameters of the link in which it is used.

Also shown in Fig. 3 are the third-order-intermodulation signals for some errors in bias point from the $c_3 = 0$ solution (the noise floor and the fundamental signals are only slightly affected by these errors). These represent cases where c_3 is opposite in sign to c_5 so the third- and fifth-degree contributions to the third-order distortion cancel at a particular PMD [15]. For PMD's above this cancellation point, the fifth-degree term dominates; below it, the third-degree term dominates. These provide higher dynamic range than the $c_3 = 0$ solution if the noise floor is above this cancellation point.

To see how the modulator behaves as a function of design, we chose values for r and ϕ_1, then determined ϕ_2 from the $c_3 = 0$ condition. The link output signals were then calculated by taking the Fourier transform of (12) with $m(v) = m_p[\sin(\omega_1 t) + \sin(\omega_2 t)]$, and the values of c_0, c_1, and M_{IP3} were calculated from the transform result. Fig. 4 shows how the modulator parameters vary with design choices. It can be sen from Fig. 4(d) that there is a solution for any value of r and ϕ_1. The modulator parameters shown in Fig. 4 completely define the modulator's performance in suboctave links, but there are several different combinations of those parameters

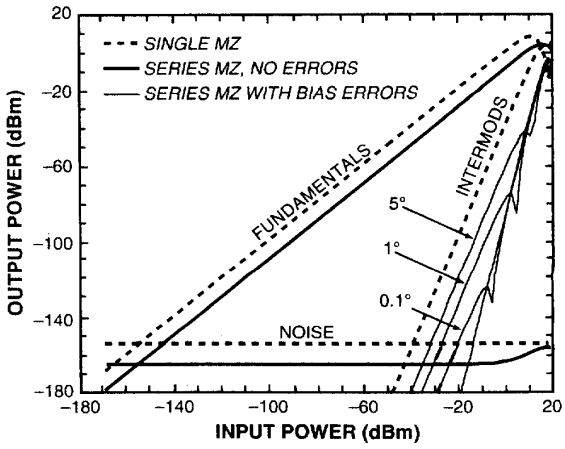

Fig. 3. Fundamental and third-order-intermodulation signals, and output noise, of links using a series interferometer (series MZ) and a single standard Mach–Zehnder interferometric modulator (single MZ). The parameters used here are $\phi_1 = 60°$, $\phi_2 = 153.61°$, $r = 3.16$ for the series MZ, and $\phi_1 = 90°$ for the single MZ. Both cases use $K_s = 100\text{W}^{-1}$ (so+10 dBm input corresponds to $m_p = 1$ for the single MZ) and $i_0 = 50$ mA; noise power is for a 1 Hz bandwidth. Also shown are the intermodulation signals for the series MZ with bias errors.

that can be significant, depending on the noise source and link performance measure that one is interested in. The average optical transmission is determined by c_0, and is a maximum for $r = 1$ and ϕ_1 near 90°. The link electrical gain is determined by $c_1^2(1+r^2)^{-1}$, which is a maximum for the same parameter values that maximize c_0. The value of M_{IP3} can become quite large, going to infinity at large r. This is *not* due to the linearization of the modulator transfer function, but is due to c_0 decreasing faster than $c_1(1+r^2)^{-0.5}$ at large r so that the optical modulation depth for a fixed PMD increases; the single MZ shows the same behavior as ϕ_1 approaches 180° [3].

Table I shows how this modulator can be optimized to excel in most systems. There are six basic optimization criteria: three possible noise sources and two link performance measures (F and DR). Equations (8), (10), and (11) have been used to determine the modulator figure of merit appropriate to each case. In the receiver-noise-limited case, the best optimization for the series MZ is $r = 1$ and ϕ_1 near 90° so $c_1^2/(1+r^2)$ is largest. In this case, the series MZ cannot provide as low a noise figure as the single MZ at quadrature (which has $c_1 = -0.5$, $r = 0$). The dynamic range of the series MZ is still larger than that of the single MZ, even though $c_0 M_{IP3}$ is smaller, because of the $n = 5$ intermodulation product slope. In the shot-noise-limited case, an optimization for the series MZ is $\phi_1 \to 180°$ with $r < 1$; $\phi_2 \to 180°$ with $r > 1$ is also an optimum choice. The noise figure is better than that of a single MZ at quadrature, showing the same 3 dB improvement as the single MZ with $\phi_1 \to 180°$. The noise figure in this limit is 13.5 dB better than that of the dual parallel MZ. The dynamic range is not only much larger than that of a single MZ, but it is also 8.6 dB larger than the dynamic range of a dual parallel MZ because $c_0 M_{IP3}^2$ is 12× larger ($r = 2$ was used for the dual parallel MZ, which gives its optimum performance). In the RIN-dominated case, the effect of the

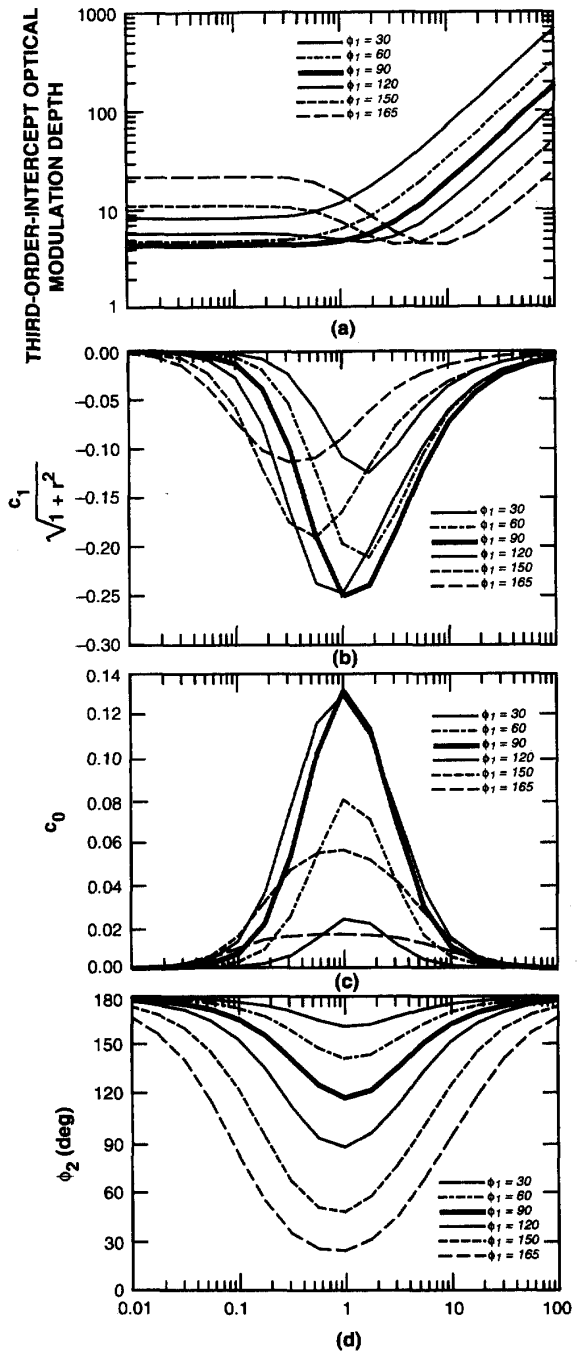

Fig. 4. Modulator design choices and their effect on modulator performance measures. The independent variable is the ratio r of phase modulation depths: (a) third-order-intercept optical modulation depth, (b) linear transfer function coefficient (normalized by total input electrical power), (c) dc transmission coefficient, and (d) second modulator bias point ϕ_2.

RIN noise term can be made arbitrarily small by optimizing the modulator parameters as described above for the shot-noise-limited case. This means that, as for the single MZ with $90° < \phi_1 < 180°$, the modulator can always be designed so that shot or thermal noise is the limiting link noise source (this does not mean that the performance level is always as good as without RIN, though). In the case where the average detector current $i_{avg} = c_0 i_0$ is limited to a fixed maximum value, examination of (8) and (10) shows that the modulator criteria for best performance are the same as for the RIN-dominated case. In real systems, more than one noise source is usually significant, but Table I helps one understand where the modulator works best.

Space does not permit plotting all of the performance measures in Table I as a function of modulator design, but we can examine the series MZ performance in a typical high-performance link. Fig. 5 shows the dynamic range, noise figure, gain, and average detector current as a function of modulator design for a link with $K_s = 100\text{W}^{-1}$, $R_d = 50\ \Omega$, no RIN, $F_R = 0$ dB, and $i_0 = 50$ mA. (Fig. 3, 5–7 also use these link parameters, except that i_0 varies in Fig. 6. A 1 km link using a 140 mW diode-pumped Nd:YAG laser, a modulator with a total insertion loss of 3 dB made with MZs having $v_\pi = 3.1$ V, a detector with 0.9 A/W responsivity, and no postamplifier would have approximately these parameters.) For r near 1, the link is shot noise dominated. At large or small r, the average detector current becomes very small, receiver noise dominates, and the link performance falls. The highest gain is achieved near $r = 1$, but the best noise figure and dynamic range are achieved away from $r = 1$.

Fig. 6 shows how a particular series MZ design ($r = 3.16$, $\phi_1 = 60°$, $\phi_2 = 153.61°$; a near-optimum choice for $i_0 = 50$ mA) compares to a single MZ for various values of i_0. The dynamic range is larger everywhere. The noise figure is smaller than for the single MZ with $\phi_1 = 90°$ at high i_0 where receiver noise is smaller than shot noise (if one were interested in using a series MZ at low i_0, a design with $r = 1$ could reduce the noise figure penalty to the 6 dB evident in Table I in the receiver-noise-limited case). The noise figure is about 1 dB worse than the single MZ biased at $\phi_1 = 157°$ (chosen because it has the same c_0 as the series MZ design). Even though the series MZ can reach the same noise figure as the single MZ with $90° < \phi_1 < 180°$ in the pure shot-noise-limited case, when both receiver noise and shot noise are present, the series MZ does not provide as good a noise figure as the single MZ with $90° < \phi_1 < 180°$. If RIN were present in this example, the noise figure of the single MZ biased at 90° would be increased by a much greater factor than that of the series MZ.

C. Tolerances and Control

The series MZ has only one critical adjustment, which is the bias point of one modulator. Fig. 4(d) shows that for any value of r or ϕ_1, there is a value of ϕ_2 that will satisfy $c_3 = 0$. The parameters r and ϕ_1 can be set approximately, then ϕ_2 can be controlled precisely (by minimizing the third harmonic of a test signal, for example). Fig. 7 shows how the dynamic range varies with an error in this critical bias point; zero error corresponds to the $c_3 = 0$ solution. For a very high dynamic range link, such as the 1 Hz bandwidth case in Fig. 7, a tiny error substantially drops the dynamic

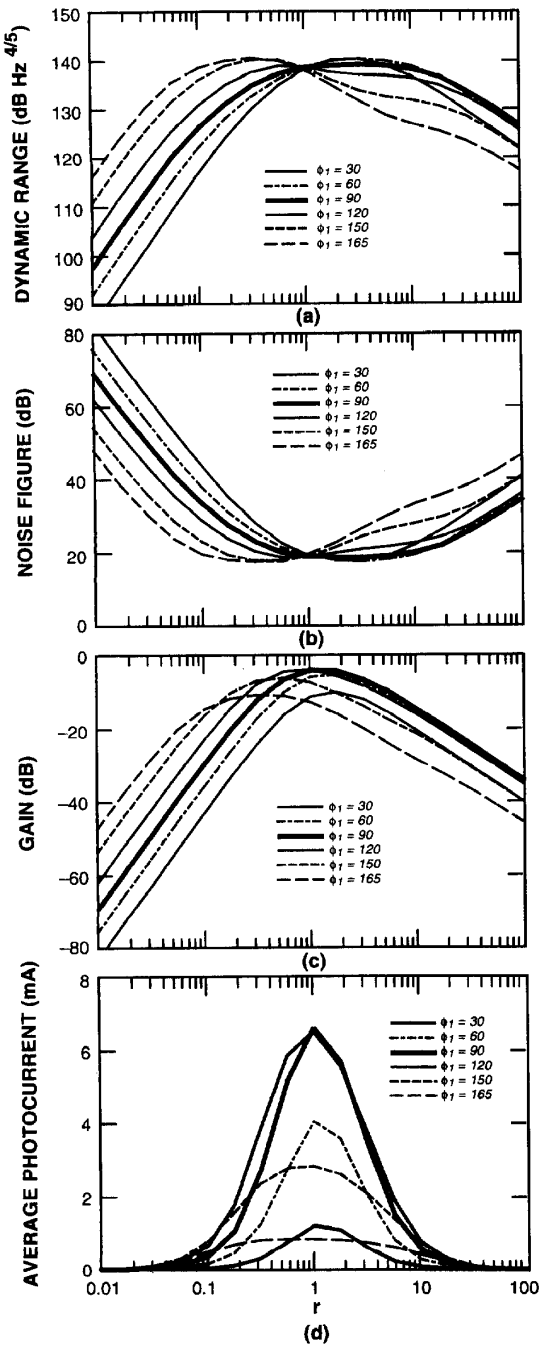

Fig. 5. Effect of modulator design on link performance: (a) third-order-intermodulation-free dynamic range, (b) noise figure, (c) electrical gain, and (d) average (i.e., dc) current from photodetector. Parameters used are $K_s = 100$ W^{-1}, $i_0 = 50$ mA, RIN=0, detector load resistance of 50 Ω, and receiver noise figure of 0 dB.

range below its peak value (0.1° error reduces dynamic range for 7 dB here). Substantial errors can be tolerated, however, while still preserving a larger dynamic range than that of a single MZ: the dynamic range of a single MZ with the link

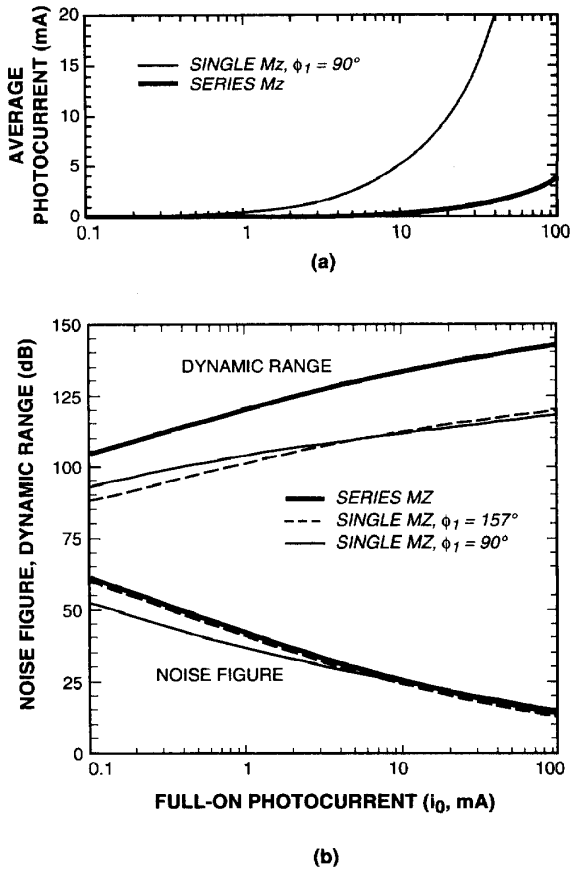

Fig. 6. Performance comparison of a link using the dual series interferometer ($\phi_1 = 60°$, $\phi_2 = 153.61°$, $r = 3.16$) with a link using the single interferometer biased at both the standard $\phi_1 = 90°$ and at $\phi_1 = 157°$ (which gives the same average photocurrent as the series interferometer here): (a) average detector photocurrent and (b) third-order-intermodulation-free dynamic range (with 1 Hz noise bandwidth) and noise figure. Link parameters (except i_0) are as for Fig. 5.

parameters used in Figs. 3 and 7 is 116.5 dB $Hz^{2/3}$. For a link with lower dynamic range, such as the 1 MHz bandwidth case in Fig. 7, the sensitivity to error is much smaller (0.5° error reduces dynamic range by $\leq$ 4 dB).

A small shift in bias point can produce a larger dynamic range than the $c_3 = 0$ bias point, as discussed above. For a very high dynamic range link, the tolerance required to take advantage of this would be a few hundredths of a degree and would not be practical; for a more modest dynamic range, where the noise floor is at a larger PMD, this solution may be practical. If a test signal is used to determine where to set the modulator bias point, its PMD must be lower than the PMD of a link signal that produces third-order-intermodulation signals above the link noise floor. If too large a PMD is used, minimizing the third harmonic of the test signal would set the bias point where the dynamic range would not be maximized for smaller-amplitude signals.

The electrical signals to the two modulators must be in phase. (For nonzero instantaneous electrical bandwidth, the

TABLE II
COMPARISON OF EXPERIMENTAL LINKS USING SERIES MZ AND SINGLE MZ MODULATORS (i_0 = 7.1mA FOR BOTH)

	AVG DET CURRENT (mA)	RF GAIN (dB)	OUTPUT NOISE (dBm/Hz)	NOISE FIGURE (dB)	DR(1) AT 1 MHz (dB)	DR,(2) NORMALIZED
SINGLE MZ	3.5	−4.5	−151.2	27.3	69.3	109.3 dB-Hz$^{2/3}$
SERIES MZ	0.94	−10.8	−157.1	27.7	87.8	132 dB-Hz$^{4/5}$
CHANGE		−6.3	−5.9	+0.4	+18.5	

(1) Maximum third-order-intermodulation-free dynamic range obtained at 1 MHz noise bandwidth. (2) DR if bias point set for uniform 5th degree intermod slope on series MZ.

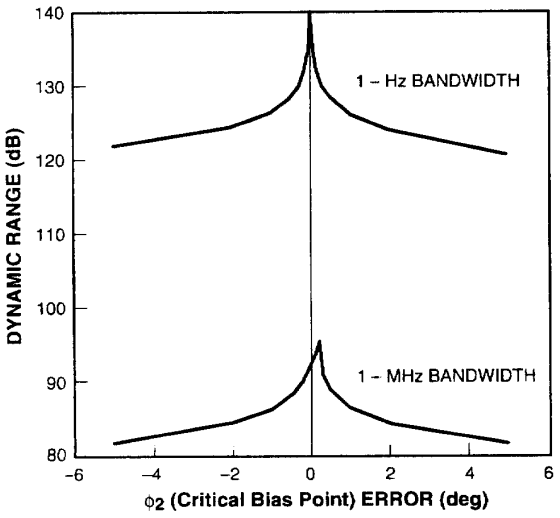

Fig. 7. Effect of errors in the critical bias point on the dynamic range. Systems with the noise floor at larger phase modulation depths (exemplified here by using a larger noise bandwidth) are less affected by errors. Parameters are the same as for the series MZ in Fig. 3. The dynamic range of a comparable link using a single MZ modulator is 116.5 dB Hz$^{2/3}$.

electrical signal to the second modulator must arrive at the same time as the light from the first modulator that was modulated by that same signal.) For modulators designed with r near 1, an electrical phase error of ±5° causes a 4 dB dynamic range decrease (in the 1 Hz bandwidth case with link parameters as in Figs. 3 and 7).

For links with nonzero instantaneous electrical bandwidth, variation in the electrical power split r^2 can reduce the dynamic range. The bias point can compensate for changes in the mean value of r^2, but not for variation across the band. As might be expected by looking at Fig. 4(d), the largest ripple in r^2 is allowed near $r = 1$. At this point, for the 1 Hz bandwidth case with link parameters as in Figs. 3 and 7, a ripple in r^2 of ±0.5 dB produces a 4 dB decrease in dynamic range.

III. EXPERIMENT

A simple link experiment was performed to verify some of the theoretical predictions. A series MZ was formed by connecting the output fiber of one interferometric modulator to the input fiber of a second nearly identical modulator. The input electrical signal was equally split between the modulators, and the electrical cable length to the second modulator was adjusted so that the electrical drive signals to the two modulators were in phase (including the effect of optical propagation delay) at all frequencies. The experimental link had approximately 11 dB of excess optical insertion loss: the 1320 nm, diode-pumped Nd:YAG laser launched 90 mW into the input fiber, the maximum detector current (both modulators at maximum transmission $\phi_1 = \phi_2 = 0°$) was 7.1 mA, and the responsivity of the 75-μm-diameter InGaAs *pin* detector was 0.95 A/W. The detector required 10 V bias to keep its nonlinearity from affecting link performance in the series-MZ link (only 5 V was required in the single-MZ link). This link was assembled from commercially obtained components; the optical insertion loss would be substantially lower ($\approx$ 4 dB) if an integrated modulator were used.

To get the performance of this link with a single MZ, the second modulator was set to $\phi_2 = 0°$ and its RF input was disconnected. The first modulator was set to approximately $\phi_1 = 90°$ to obtain $i_{avg} = 3.5$ mA. The two-tone (530 and 531 MHz) third-order intermodulation distortion was measured using two synthesizers and a spectrum analyzer. The output noise level was measured by using a low-noise amplifier (not used in the distortion measurement) after the detector. The results are summarized in the first line of Table II.

To see the link performance with the series MZ, the second modulator's electrical drive was reconnected and its bias point was set to minimize the third-order distortion at a 1 MHz noise bandwidth. This occurred at a bias point of $\phi_2 \approx 118°$; the average detector current was $i_{avg} = 0.94$ mA. The results from this case are summarized in the second line of Table II. The bias point used for this measurement corresponds to a slight deviation from a uniform 5th-degree slope, as required for maximum dynamic range at the 1 MHz noise bandwidth (refer to Figs. 3 and 7). We were able to move the local minimum in the intermodulation products to higher modulation depths by varying the bias point ϕ_2, as expected from Fig. 3. We were not able to obtain the uniform 5th-degree slope ($c_3 = 0$ condition) because distortion in the spectrum analyzer prevented accurate bias point control with the small-modulation-depth

pilot tone required to maintain this condition. The 132 dB-$Hz^{4/5}$ dynamic range shown in Table II was therefore obtained by extrapolating from the larger modulation depths in our measurement where the intermodulation products did vary as the 5th degree of the input power.

Using the theory described in Section II, a link with the parameters of the experimental series MZ link ($i_0 = 7.1$ mA, $r = 1$, $\phi_1 = 90°$, $R_d = 425\ \Omega$, $K_s = 136\ W^{-1}$, $\mathcal{R} \leq -175$ dB/Hz, $F_R = 1.41$) should have $c_3 = 0$ when $\phi_2 = 118.073°$. This link should have $i_{avg} = 0.94$ mA, $G = -10.4$ dB, $N_o = -158.8$ dBm/Hz, $F = 25.6$ dB, and $DR = 132$ dB$-Hz^{4/5}$. By comparing these numbers to those in Table II, it can be seen that the theoretical prediction is very close to reality. For the single-MZ link, the theoretical prediction is $i_{avg} = 3.5$ mA, $G = -4.4$ dB, $N_o = -153.1$ dBm/Hz, $F = 25.3$ dB, and $DR = 111$ dB$-Hz^{2/3}$. The only significant difference between theory and experiment is in the noise level N_o (this causes the noise figure errors); since this difference is the same for both links, it is probably just a calibration error in the noise level measurement.

The close agreement of calculated and measured results, along with the qualitative agreement between Fig. 3 and the observed behavior of the intermodulation signals with changes in ϕ_2, is good evidence that the theoretical calculations presented in Section II are valid.

IV. Summary

We have shown how a linearized modulator can be designed for suboctave analog links that provides substantial third-order-intermodulation-free dynamic range improvement with little noise figure penality. The only critical adjustment is a single bias point, and the tolerances required are within practical limits. This modulator design has the advantages obtainable by biasing a single interferometric modulator near its minimum transmission point: the average detector current can be drastically reduced, and the noise figure can be better than that of a comparable link using a single interferometric modulator biased at quadrature when shot noise or RIN is the dominant link noise source. This modulator can be realized simply by connecting two standard fiber-coupled interferometric modulators together in series (with polarization control between them), although lower optical insertion loss is possible by integrating both interferometers on a single chip as is shown in Fig. 2. A simple experiment has verified some of the key theoretical predictions about this modulator.

Acknowledgment

The author would like to acknowledge F. J. O'Donnell for assistance in performing the series modulator experiment.

References

[1] G. E. Betts, L. M. Johnson, and C. H. Cox, III, "Optimization of externally modulated analog optical links," *Proc. SPIE*, vol. 1562, pp. 281–302, 1991.
[2] G. E. Betts and F. J. O'Donnell, "Improvements in passive, low-noise-figure optical links," presented at Photon. Syst. Antenna Appl. III, Jan. 20–22, 1993.
[3] M. L. Farwell, W. S. C. Chang, and D. R. Huber, "Increased linear dynamic range by low biasing the Mach–Zehnder modulator," *IEEE Photon. Technol. Lett.*, vol. 5, pp. 779–782, 1993.
[4] G. E. Betts, "A linearized modulator for high performance bandpass optical analog links," in *1994 IEEE MTT-S Int. Microwave Symp. Dig.*, 1994, pp. 1097–1100.
[5] M. L. Farwell, Z. Q. Lin, E. Wooten, and W. S. C. Chang, "An electrooptic intensity modulator with improved linearity," *IEEE Photon. Technol. Lett.*, vol. 3, pp. 792–795, 1991.
[6] W. B. Bridges and J. H. Schaffner, "Review of linearized integrated optic modulators for fiber optic links," presented at Photon. Syst. Antenna Appl. IV, Jan. 18–21, 1994.
[7] S. K. Korotky and R. M. DeRidder, "Dual parallel modulation schemes for low-distortion analog optical transmission," *IEEE J. Select. Areas Commun.*, vol. 8, pp. 1377–1380, 1990.
[8] L. M. Johnson and H. V. Roussell, "Reduction of intermodulation distortion in interferometric optical modulators," *Opt. Lett.*, vol. 13, pp. 928–930, 1988.
[9] P. L. Liu, B. J. Li, and Y. S. Trisno, "In search of a linear electrooptic amplitude modulator," *IEEE Photon. Technol. Lett.*, vol. 3, pp. 144–146, 1991.
[10] H. Skeie and R. V. Johnson, "Linearization of electro-optic modulators by a cascade coupling of phase modulating electrodes," *Proc. SPIE*, vol. 1583, pp. 153–164, 1991.
[11] Y. Wang-Boulic, "A linearized optical modulator for reducing third-order intermodulation distortion," *J. Lightwave Technol.*, vol. 10, pp. 1066–1070, 1992.
[12] G. J. McBrien and J. D. Farina, "Cascaded optic modulator arrangement," U.S. Patent 5,168,534, 1992.
[13] J. H. Schaffner and W. B. Bridges, "Intermodulation distortion in high dynamic range microwave fiber-optic links with linearized modulators," *J. Lightwave Technol.*, vol. 11, pp. 3–6, 1993.
[14] T. R. Halemane and S. K. Korotky, "Distortion characteristics of optical directional coupler modulators," *IEEE Trans. Microwave Theory Tech.*, vol. 38, pp. 669–673, 1990.
[15] A. Djupsjöbacka, "A linearization concept for integrated-optic modulators," *IEEE Photon. Technol. Lett.*, vol. 4, pp. 869–872, 1992.

Gary E. Betts was born May 14, 1954, in Seattle, WA. He received the B.S. degree in physics from Haverford College, Haverford, PA, and the M.S. degree in physics and the Ph.D. degree in applied physics from the University of California at San Diego in 1976, 1980 and 1985, respectively.

From 1976 to 1978, he worked in integrated optics, primarily on the design of geodesic lenses, at the Westinghouse Electric Corporation, Baltimore, MD. Since 1985, he has been a staff member at the Massachusetts Institute of Technology, Lincoln Laboratory, Lexington, MA, working on lithium niobate integrated-optical devices. His work at MIT has included development of externally modulated optical analog links, microwave-frequency modulators, low-frequency modulators with very high sensitivity, linearized modulators, and investigation of optical damage in lithium niobate.

Dr. Betts is a member of the Optical Society of America and the IEEE Lasers and Electro-Optics Society.